Palladium-Catalyzed C–S Bond Formation: Rate and Mechanism of the Coupling of Aryl or Vinyl Halides with a Thiol Derived from a Cysteine

Xavier Moreau,[a] Jean Marc Campagne,*[a] Gilbert Meyer,[b] and Anny Jutand*[b]

Keywords: Palladium / C–S coupling / Reaction mechanisms / Kinetics / Atropisomerism

The mechanism of the palladium-catalyzed coupling reaction of aryl or vinyl halides with a thiol derived from a protected chiral cysteine **1** (RSH), leading to C–S bond formation, has been investigated in the context of catalytic reactions. All palladium complexes involved in the catalytic cycle have been characterized, successively, as PhPdI(dppf), PhPdI(SHR)(η^1-dppf) and PhPd(SR)(dppf). The oxidative addition reaction which generates PhPdI(dppf) is followed by the metallation of **1** whose mechanism has been investigated. In the case of the weakly acidic cysteine **1** (RSH) studied here, the anions RS^- are not generated in detectable concentrations in the reaction with the NEt_3 base. Even if the classical transmetallation reaction of PhPdI(dppf) by RS^-, present at a very low concentration, cannot be entirely excluded, we propose that an alternative mechanism, complexation of the thiol, leads to the previously unreported PhPdI(SHR)(η^1-dppf) (observed by ^{31}P NMR spectroscopy) after decomplexation of one of the phosphorus atoms of the dppf ligand, followed by the easier deprotonation of the coordinated RSH by the base, which generates PhPd(SR)(dppf). A classical reductive elimination reaction delivers the coupling product PhSR. The kinetics of all the steps have been investigated independently, one after the other, starting from $Pd_2(dba)_3$ and dppf, using the initial concentrations of the reagents used in the catalytic reaction. Under the experimental conditions used in the catalytic reaction involving phenyl iodide and NEt_3 as the base, the reductive elimination reaction is the slowest step which mainly limits the rate of the catalytic cycle up to approximately 80 % conversion. The metallation reaction of RSH is very slow when propylene oxide was used as the probase. The reductive elimination is the slowest step in the cross-coupling of a vinyl iodide. Diastereoisomers of the vinyl-PdX(dppf) (X = I, SR) complexes were observed as a result of the atropisomerism induced by the bulkiness of the investigated vinyl group and the chiral center present on the vinyl or on the SR group.

Introduction

In an ongoing project towards the total synthesis of Griseoviridin, it was planned to construct the nine-membered thiolactone by a palladium-catalyzed cross-coupling reaction of a vinyl iodide with a thiol derived from a D-cysteine (Scheme 1).[1,2]

In this context, the palladium-catalyzed cross-coupling reaction of vinyl or aryl halides with a cysteine-derived thiol

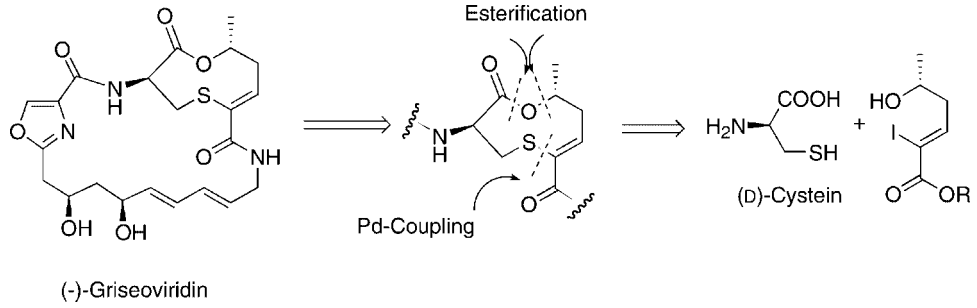

Scheme 1. Retrosynthesis of (–)-Griseoviridin.

[a] Institut de Chimie des Substances Naturelles,
Avenue de la Terrasse, Bat. 27, 91198 Gif Sur Yvette, France
E-mail: Jean-Marc.Campagne@icsn.cnrs-gif.fr
[b] Ecole Normale Supérieure, Département de Chimie, UMR CNRS-ENS-UPMC 8640
24 Rue Lhomond, 75231 Paris Cedex 5, France
Fax: +33-1-4432-3325
E-mail: Anny.Jutand@ens.fr

1 has been optimized (Scheme 2).[1,2] The most efficient Pd^0 precursor is $Pd^0_2(dba)_3{\cdot}CHCl_3$ (dba = *trans*,*trans*-dibenzylideneacetone) associated with the bidentate ligand dppf [1,1′-bis(diphenylphosphanyl)ferrocene].[3–5]

When considered independently of each other, each step in a catalytic cycle has its own reaction rate. But in a cata-

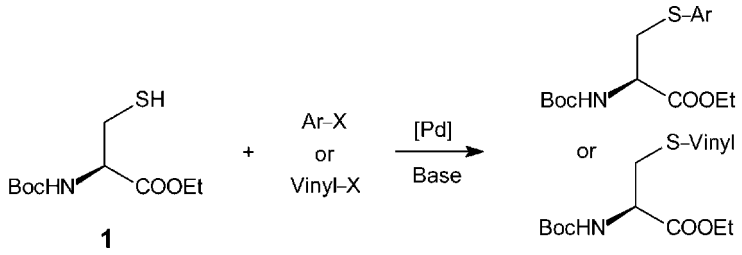

Scheme 2. Pd-catalyzed cross-coupling reaction of aryl or vinyl halides with a cysteine-derived thiol **1**.

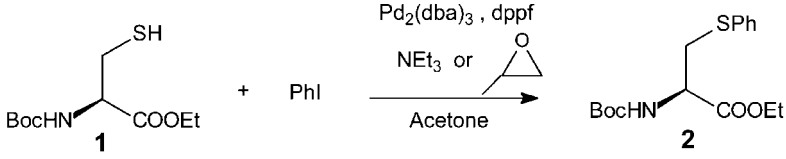

Scheme 3. Pd-catalyzed cross-coupling reacion of phenyl iodide with cysteine-derived thiol **1**.

lytic cycle, these steps have the same rate because of the steady-state requirement.[6] It would, however, be of interest to investigate the kinetics of each step in a catalytic cycle independently of each other to determine the intrinsically slowest reaction that mainly limits the rate of the catalytic cycle. We report herein the mechanism of the cross-coupling reactions shown in Scheme 2. The rate and mechanism of each step of the catalytic cycle have been investigated separately, one after the other, under the experimental conditions used in the catalytic reactions, starting from the same precursor, the same ligand and the same solvent.

Results and Discussion

Mechanism of the Palladium-Catalyzed Cross-Coupling Reaction of Phenyl Iodide with the Cysteine-Derived Thiol 1

The cross-coupling reaction reported in Scheme 3[2] gives the sulfide **2** in refluxing acetone in 79% yield in the presence of NEt_3 and in 47% yield in the presence of propylene oxide. The mechanism of this catalytic reaction has been elucidated by means of electrochemical techniques combined with ^1H and ^{31}P NMR spectroscopy performed in acetone.

The Rate and Mechanism of the Oxidative Addition of Phenyl Iodide to Palladium(0) Generated from $Pd_2(dba)_3$·$CHCl_3$ and dppf (Pd/dppf = 1) in Acetone

The reaction of $Pd_2(dba)_3$·$CHCl_3$ and dppf (Pd/dppf = 1) in acetone was monitored by ^{31}P NMR spectroscopy and cyclic voltammetry. The air-sensitive $Pd^0(dba)(dppf)$ was quantitatively generated five minutes after mixing (as in the reaction of $Pd(dba)_2$[7a] with 1 equiv. of dppf)[7b] and characterized by two doublets: 17.7 (1 P, J_{PP} = 9 Hz) and 20.1 ppm (1 P, J_{PP} = 9 Hz) (Scheme 4).[7b]

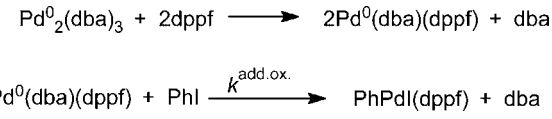

Scheme 4.

The complex $Pd^0(dba)(dppf)$ completely disappeared after the addition of 1.1 equiv. of PhI, which led to the quantitative formation of PhPdI(dppf), characterized by two doublets at 7.7 (d, J_{PP} = 34 Hz, 1 P) and 26.2 ppm (d, J_{PP} = 34 Hz, 1 P), similar to those of an authentic sample (Scheme 4).[7b] The mechanism of the oxidative addition of PhI to the Pd^0 complex generated from $Pd^0(dba)_2$ and dppf (Pd/dppf = 1) has already been established in THF.[7b] The major complex $Pd^0(dba)(dppf)$ is involved in an endergonic equilibrium with dba and the minor complex $SPd^0(dppf)$ (*S* = Solvent). Both complexes are reactive in the oxidative addition reaction, $SPd^0(dppf)$ being the most reactive (Scheme 5).[7b]

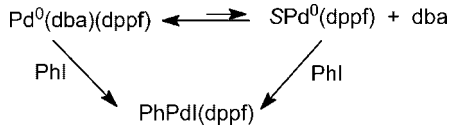

Scheme 5. Oxidative addition of PhI to the Pd^0 complexes generated from $Pd^0{}_2(dba)_3$ or $Pd^0(dba)_2$ and dppf (Pd/dppf = 1 in both cases).

As demonstrated in earlier work,[7b] dba plays a crucial role (Scheme 5) since the overall reactivity is controlled by the dba concentration which differs according to the precursor employed, $Pd_2(dba)_3$·$CHCl_3$ or $Pd(dba)_2$. Since our objective is to compare the rate of each step in the context of the experimental conditions used in the catalytic reaction, the kinetics of the oxidative addition of PhI has been re-investigated in acetone by electrochemical techniques[7b]

by using $Pd_2(dba)_3{\cdot}CHCl_3$ as the precursor and the same initial concentrations as in the catalytic reaction: $Pd_2(dba)_3{\cdot}CHCl_3$ (2 mM), dppf (4 mM) and PhI (77.3 mM).[2] The complex $Pd^0(dba)(dppf)$, which was generated in acetone containing nBu_4NBF_4 (0.3 M), was characterized by an irreversible bielectronic oxidation peak at E^p_{O1} = +0.535 V versus SCE (cyclic voltammetry at a steady gold disk electrode with a scan rate of 0.5 V s^{-1}). The kinetics of the oxidative addition of PhI (77.3 mM) was monitored by amperometry at a rotating gold disk electrode polarized at +0.55 V on the plateau of the oxidation wave O_1. The decrease in the oxidation current i_t of $Pd^0(dba)(dppf)$ (proportional to its concentration) was recorded versus time after the addition of PhI up to 100% conversion. The plot of ln x versus time was linear (Figure 1) [$x = [Pd^0]_t/[Pd^0]_0 = i_t/i_0$, with i_t the oxidation current of $Pd^0(dba)(dppf)$ at time t and i_0 the initial oxidation current of $Pd^0(dba)(dppf)$]. The observed rate constant $k_{obs}^{ox.add.}$ for the overall oxidative addition reaction (Scheme 4) was determined from the slope of the straight line, $\ln x = -k_{obs}^{ox.add.}t$, to be 1.3×10^{-3} s^{-1} ([PhI] = 77.3 mM, [Pd^0] = 4 mM, acetone, 30 °C).

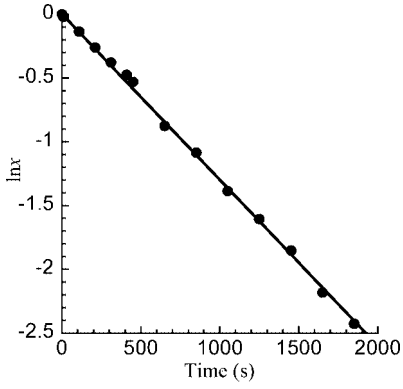

Figure 1. Kinetics of the oxidative addition of PhI (77.3 mM) to the Pd^0 complexes generated from $Pd_2(dba)_3$ (2 mM) and dppf (4 mM) in acetone containing nBu_4NBF_4 (0.3 M) at 30 °C, followed by amperometry at a rotating gold disk electrode (d = 2 mm, ω = 105 rad s^{-1}) polarized at +0.55 V on the plateau of the oxidation wave of $Pd^0(dba)(dppf)$. Plot of ln x versus time [$x = i_t/i_0$; i_t is the oxidation current of $Pd^0(dba)(dppf)$ at time t and i_0 is the initial oxidation current of $Pd^0(dba)(dppf)$]. Ln $x = -k_{obs}^{ox.add.}t$; y = –0.0012997x, R = 0.9994.

The apparent rate constant, $k_{app}^{add.ox.}$, for the overall oxidative addition reaction was also determined and a value of 0.017 $M^{-1}s^{-1}$ ([Pd^0] = 4 mM, acetone, 30 °C) was obtained.[8a]

At this level, the first step of the catalytic cycle has been fully characterized: i) the complex formed in the oxidative addition of PhI to $Pd_2(dba)_3{\cdot}CHCl_3$ and dppf (Pd/dppf = 1) is PhPdI(dppf); ii) the observed rate constant for the oxidative addition reaction, $k_{obs}^{ox.add.}$, has been determined in acetone at 30 °C for the initial PhI concentration used in the catalytic reaction.[8b]

Rate and Mechanism of the Reaction between PhPdI(dppf) and the Cysteine-Derived Thiol 1 in the Presence of NEt_3 in Acetone

The transmetallation reaction between ArPdX(dppf) complexes and thiolates R′S^-, which gives ArPd(SR′)(dppf), has been investigated by Hartwig and co-workers (Scheme 6).[9] The thiolates R′S^- were independently synthesized by reacting thiols R′SH with an appropriate base. The kinetics of the transmetallation reaction have not been investigated.

Scheme 6. Transmetallation reaction between ArPdX(dppf) complexes and thiolates.

In the present case, the ^1H NMR spectrum of the cysteine-derived thiol **1** (RSH) in [D_6]acetone was not modified by the addition of 1 equiv. of the base NEt_3. This suggests that the thiolate of the cysteine derivative **1** could not be generated in high concentrations by deprotonation with NEt_3, as predicted by their respective pK_a values.[10] Even if a classical transmetallation step between ArPdX(dppf) and RS^-, generated at a very low concentration, cannot be entirely excluded, a detailed investigation of the reaction revealed an alternative mechanism which could by-pass the endergonic formation of the free thiolate. This overall step, in which the thiol is converted into the ArPd(SR)(dppf) complex, will be denoted by the term "metallation of the thiol" (with an overall rate constant $k^{"met."}$) to distinguish it from the mechanism involving the anion RS^-.

The mechanism of the metallation of the thiol was investigated starting from the complex PhPdI(dppf) **3** (13.3 mM), quantitatively generated in situ in the stoichiometric oxidative addition of PhI to the Pd^0 complexes generated from $Pd_2(dba)_3{\cdot}CHCl_3$ and dppf (Pd/dppf/PhI = 1:1:1, 13.3 mM each) in [D_6]acetone. PhI was used in stoichiometric amounts to avoid any interference of the Pd^0 generated in later steps. When the oxidative addition reaction was over, NEt_3 (1.1 equiv.) was added to PhPdI(dppf) (**3**). NEt_3 did not react with **3**, as shown by ^{31}P NMR spectroscopy. Addition of the thiol **1** (1 equiv.) to the mixture of **3** and NEt_3 resulted in a fast reaction (reaction time of less than 20 min). The protonated amine, $HNEt_3^+$, was observed in the ^1H NMR spectrum, indicating that the RSH **1** had been deprotonated. In the ^{31}P NMR spectrum, the two doublets arising from **3** had completely disappeared and two new doublets were observed at δ = 13.4 (d, J_{PP} = 32 Hz, 1 P) and 23.4 ppm (d, J_{PP} = 32 Hz, 1 P). These were assigned to the complex PhPd(SR)(dppf) (**4**), whose structure was confirmed by ^1H NMR spectroscopy (Scheme 7).

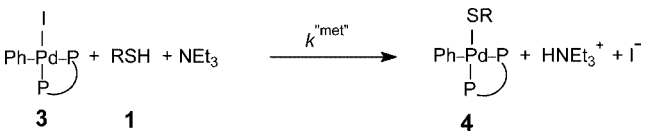

Scheme 7. Overall metallation reaction of the cysteine-derived thiol **1** in the presence of NEt_3 (P–P = dppf).

Interestingly, when 25 equiv. of the cysteine-derived thiol **1** were added to PhPdI(dppf) (13.3 mM), the two doublets from PhPdI(dppf) were still detected but two new minor singlets of similar magnitude appeared at δ = –17.9 and 18.7 ppm with a ratio 10:1 in favor of PhPdI(dppf). In the presence of 50 equiv. of **1**, this ratio decreased to 3.3:1. The former singlet is close to that of the free dppf ligand (δ = –17.6 ppm). This suggests that a reaction between PhPdI(dppf) and the thiol **1** takes place to give in an endergonic equilibrium a new complex in which one of the phosphorus atoms of the dppf ligand is displaced by the thiol **1**, as in complex **5** (Scheme 8). Although dppf is a bidentate ligand, the high P–Pd–P bite angle (ca. 99°) allows the decomplexation of one of the phosphorus atoms.

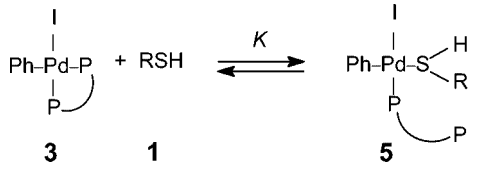

Scheme 8. Reaction between PhPdI(dppf) and the cysteine-derived thiol **1** (RSH).

The configuration of complex **5** was not determined. Indeed, such a complex could not be isolated because it was generated in an endergonic equilibrium in the presence of a large excess of RSH. Precipitation of this complex in the absence of RSH immediately resulted in the release of RSH by recomplexation of the relegated phosphorus atom in a more favored intramolecular reaction. The equilibrium constant K = [**5**]/([**3**][**1**]) (Scheme 8) was estimated from the respective magnitudes of the ^{31}P NMR signals of complexes **3** and **5** to be 0.40 ± 0.07 M^{-1} (acetone, 25 °C)

The substitution of a more labile phosphane such as PPh_3 by the cysteine-derived thiol **1** was tested with *trans*-PhPdI(PPh_3)$_2$ (**6**). The intensity of the ^{31}P NMR singlet of complex **6** in acetone (δ =23.04 ppm) decreased after the addition of 5 equiv. of the thiol **1**. Two new singlets of equal magnitude were detected, one at –5.5 ppm, characteristic of free PPh_3, and a second one at δ = 23.30 ppm assigned to complex **7** (Scheme 9).

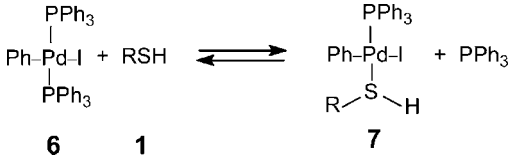

Scheme 9. Reaction between *trans*-PhPdI(PPh_3)$_2$ and the cysteine-derived thiol **1**.

When NEt_3 (1 equiv.) was added to a solution of complexes **3** and **5** in equilibrium in acetone, their ^{31}P NMR signals disappeared and only the two doublets arising from **4** were detected. Consequently, the metallation of the thiol might proceed via complex **5** by deprotonation of the ligated thiol with NEt_3, the coordinated thiol being more acidic that the free one (Scheme 10).

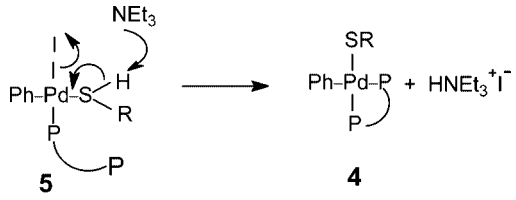

Scheme 10. Tentative mechanism for the formation of PhPd(SR)(dppf) **4** (SR = thiolate derived from the cysteine **1**).

Therefore, metallation of the thiol (Scheme 7) may proceed in two steps: complexation of the cysteine-derived thiol **1** by **3** (Scheme 8) followed by the easier deprotonation of the ligated thiol (Scheme 10) to give the transmetallation complex **4**. This overall step, characterized by the rate constant $k^{\text{"met."}}$ (Scheme 7), was too fast to be monitored accurately by ^{31}P NMR spectroscopy. The observed rate constant $k_{obs}^{\text{"met."}}$ was thus estimated after addition of a stoichiometric amount of NEt_3 and **1** (1 equiv. each) to a solution of **3** (13.3 mM), generated in situ by the oxidative addition of PhI to $Pd_2(dba)_3{\cdot}CHCl_3$ and dppf (Pd/dppf/PhI = 1:1:1, 13.3 mM each) in [D_6]acetone. Twenty minutes after mixing, the two ^{31}P NMR doublets of the transmetallation complex **4** were observed but not those of PhPdI(dppf). A minimum value of the observed rate constant, $k_{obs}^{\text{"met."}}$ (in s^{-1}), for the overall metallation step from PhPdI(dppf) (Scheme 7) could then be estimated:[11a,11b] $k_{obs}^{\text{"met."}} > 5 \times 10^{-3}$ s^{-1} ([NEt_3] = [**1**] = 13.3 mM, acetone, 25 °C).

This kind of metallation step (complexation/deprotonation) is also a key step in the palladium-catalyzed cross-coupling reaction between an aryl halide and an amine[12a,12b] in which the amine RR′NH ligated to the Pd^{II} center in ArPdXL(RR′NH) complexes is more easily deprotonated by the base. Similarly, the easier deprotonation of an alcohol ROH ligated to a Pd^{II} center in ArCO–PdXL(ROH) complexes is also proposed as a key step in the palladium-catalyzed synthesis of ArCOOR from ArX, CO and ROH.[12c]

Kinetics of Reductive Elimination from PhPd(SR)(dppf) (4)

Even if a large number of rate constants for reductive elimination reactions have been reported,[9] none of them concerns the SR group derived from **1**. Moreover, in contrast to the present work, the rate of the reductive elimination has not been compared to the rate of the preceding steps: the oxidative addition and transmetallation reactions involved in the catalytic reaction.[9a] The kinetics of the reductive elimination from complex **4** (Scheme 11), which gives the cross-coupling product **2** (Scheme 3), were thus investigated. Complex **4** was generated as above, by reacting NEt_3 and **1** with PhPdI(dppf) (13.3 mM) generated in situ from $Pd_2(dba)_3$ and dppf under stoichiometric conditions: Pd/dppf/PhI/NEt_3/**1** = 1:1:1:1:1.[13] The reductive elimination reaction was slow enough to be followed by ^{31}P NMR spectroscopy by monitoring the decrease in the intensity of the doublets of **4** relative to the intensity of the sing-

let of H_3PO_4 (85% in water) introduced into the capillary tube as an internal standard.

Scheme 11. Reductive elimination from complex **4** (P–P = dppf, SR = deprotonated thiol **1**).

The plot of $\ln r$ versus time is linear (r is the ratio of the magnitude of one doublet of **4** to the magnitude of the singlet of the standard at time t) (Figure 2). The rate constant for the reductive elimination reaction was determined from the slope: $\ln r = -k^{red.elim.}t + \ln r_0$. A value of $k^{red.elim.} = 2.3 \times 10^{-4}$ s^{-1} (acetone, 25 °C) was determined.

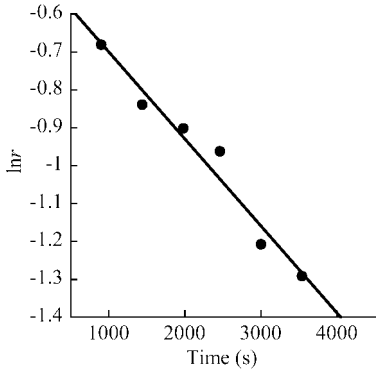

Figure 2. Kinetics of the reductive elimination from PhPd(SR)(dppf) (**4**) in acetone to give the cross-coupling product **2**, as monitored by ^{31}P NMR spectroscopy at 25 °C. Plot of $\ln r$ (r is the ratio of the magnitude of one doublet of **4** to the magnitude of the singlet of the internal standard) versus time. $\ln r = -k^{red.elim.}t + \ln r_0$; $y = -0.47044 - 0.00022973x$, $R = 0.9814$.

When the reaction was performed in [D$_6$]acetone with the complex **3** generated by the oxidative addition of PhI, used in slight excess (1.5 equiv.) relative to $Pd_2(dba)_3{\cdot}CHCl_3$ and dppf (Pd/dppf/PhI/**1**/NEt$_3$ = 1:1:1.5:1:1), the Pd^0 complex formed in the reductive elimination from complex **4** (Scheme 11) again underwent oxidative addition with the excess PhI, as attested by the detection of the two ^{31}P NMR doublets arising from PhPdI(dppf). Figure 3 shows the coexistence of i) remaining complex PhPd(SR)(dppf) (**4**) that has not yet undergone reductive elimination, ii) the complex Pd^0(dba)(dppf) recycled in the reductive elimination reaction (Scheme 11) and iii) the complex PhPdI(dppf) (**3**) that has been generated in the oxidative addition of excess PhI to Pd^0(dba)(dppf) and Pd^0(dppf) before the reductive elimination was over. This establishes the fact that the first catalytic cycle has been closed (Scheme 12) and that the second cycle has started before the total conversion of PhPd(SR)(dppf) in the slow reductive elimination.

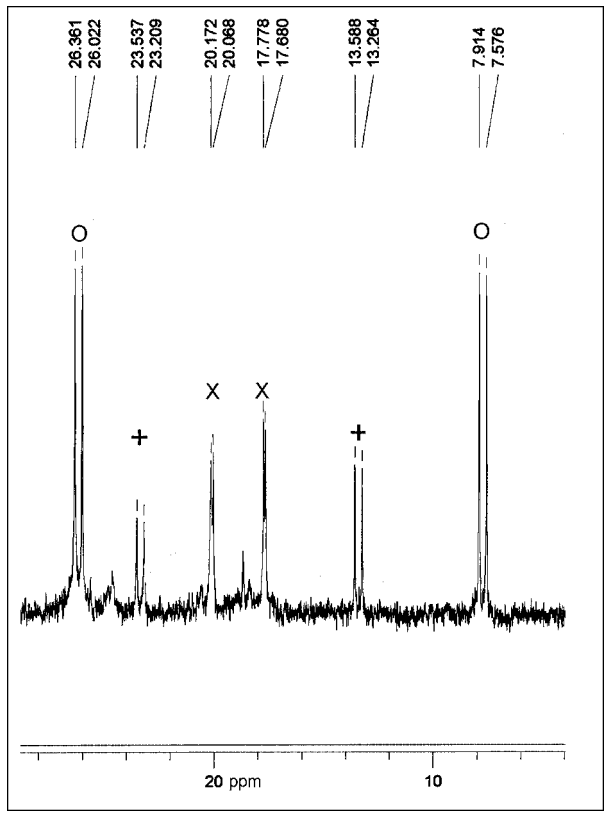

Figure 3. ^{31}P NMR spectra (101 MHz, [D$_6$]acetone) of (+) PhPd(SR)(dppf) **4** (SR: thiolate derived from **1**), (○) PhPdI(dppf) **3** and (×) Pd^0(dba)(dppf) observed during the reductive elimination step (almost over) from the reaction of **1** and NEt$_3$ with PhPdI(dppf), previously generated in the oxidative addition of PhI (in slight excess) to $Pd_2(dba)_3{\cdot}CHCl_3$ and dppf (Pd/dppf/PhI/**1**/NEt$_3$ = 1:1:1.5:1:1).

Mechanism of the Cross-Coupling Reaction

A mechanism of the palladium-catalyzed cross-coupling reaction between PhI and the cysteine-derived thiol **1** in the presence of NEt$_3$, which leads to **2** (Scheme 3), has been proposed in which all the intermediate complexes have been characterized (Scheme 12). Moreover, the kinetics of each step have been investigated separately, one after another. By considering the concentration of the reactive palladium complex in each step taken independently to be the same, we can compare the values of $k_{obs}^{ox.add.}$, $k_{obs}^{"met."}$ and $k^{red.elim.}$ (all expressed in s^{-1} and determined by using the same initial reagent concentrations as used in the catalytic reaction: [PhI] = 77.7 mM, [**1**] = 107 mM, [NEt$_3$] = 155 mM and [Pd^0] = 4 mM[2]) and thus determine which step is the slowest.[14a–14c] The kinetics of the oxidative addition reaction were investigated by using the initial concentrations of the catalytic reaction (vide supra). By comparing the values of $k^{red.elim.}$ and $k_{obs}^{ox.add.}$ (2.3×10^{-4} and 1.3×10^{-3} s^{-1}, respectively), we can assume that, when considered independently, the reductive elimination is slower than the oxidative addition for the initial PhI concentration used in the catalytic reaction.[14a,14b]

Since the metallation of **1** was fast, its kinetics were investigated under stoichiometric conditions with [**1**] = [NEt$_3$]

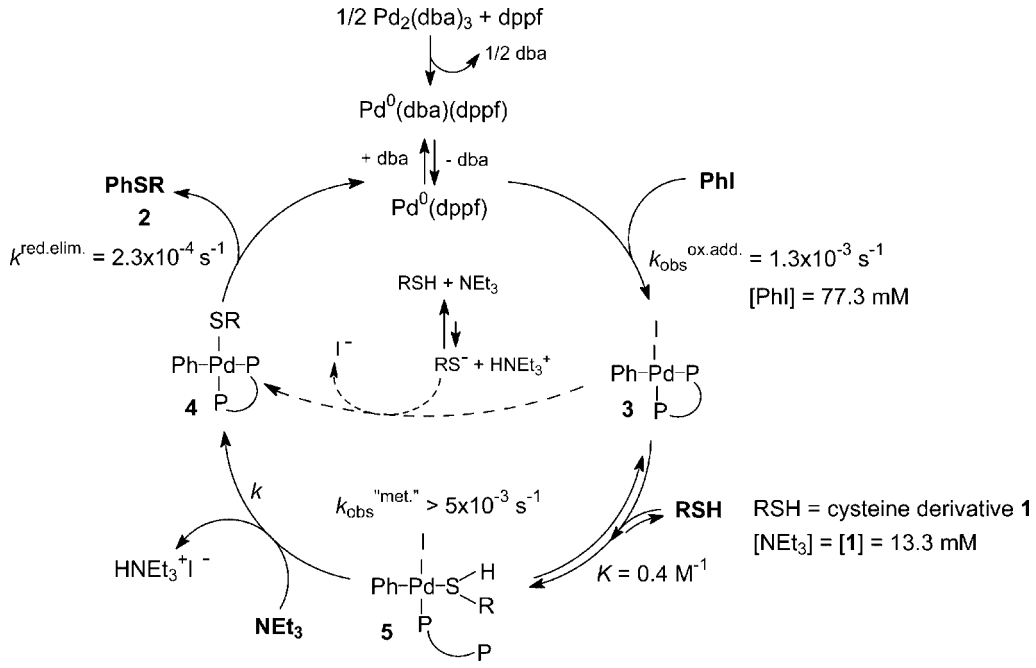

Scheme 12. Mechanism of the palladium-catalyzed cross-coupling reaction between phenyl iodide and the cysteine-derived thiol **1** in acetone (Scheme 3). $k_{obs}^{add.ox.}$ was determined for [Pd] = 4 mM. For the metallation and reductive elimination steps investigated separately, [**3**] = [**4**] = 13.3 mM.

= 13.3 mM, that is, with concentrations lower than the initial ones used in the catalytic reaction (vide supra).[2] Consequently, the value of the observed rate constant, $k_{obs}^{"met."}$, will be much higher than the minimum value of 5×10^{-3} s^{-1} estimated in this work, when considering the initial reagent concentrations used in the catalytic reaction.[11b,14c]

Therefore, from the values of the observed rate constants for the oxidative addition ($k_{obs}^{ox.add.} = 1.3 \times 10^{-3}$ s^{-1}), the metallation ($k_{obs}^{"met."} > 5 \times 10^{-3}$ s^{-1}) and the reductive elimination ($k^{red.elim.} = 2.3 \times 10^{-4}$ s^{-1}) reactions determined in this work, and with the concentration of the active palladium complex the same in each independent step, one observes that for the reagent concentrations given in Scheme 12 and those used in the catalytic reaction, the reductive elimination reaction is the slowest step that mainly controls the rate of the catalytic cycle.

However, the step that determines the rate of the catalytic cycle may change as the catalytic reaction proceeds. Indeed, since the PhI concentration decreases during the catalytic reaction, the oxidative addition reaction may become slower than the reductive elimination reaction whose intrinsic rate does not depend on the reagent concentrations but only on the concentration of **4**.[14a] The intrinsic rates of the reductive elimination and the oxidative addition reactions, taken independently, are similar at 82% conversion under the experimental conditions of the catalytic reaction.[14d] Beyond this, the rate of the catalytic cycle will be controlled by the oxidative addition reaction.

Having obtained the values of the rate constants for the reductive elimination (determined above), the oxidative addition[8a] and the metallation steps,[11c] the concentration profiles of the reagents, products and catalytic species have been simulated by means of the AnaCin2000 program using the initial concentrations of PhI, NEt_3, RSH **1** and Pd^0 employed in the catalytic reactions, (Figure 4a, see ref.[15] for the simulated kinetic scheme).

Zooming in on the low concentration range (0–0.005 M) reveals the concentration profiles of the catalytic species as the catalytic reaction proceeds (Figure 4b). Complexes **3** and **5** are hardly detected indicating that they are present at concentrations of less than 10^{-4} M because they are involved in the fast steps (complexation and deprotonation, respectively), as predicted from our experimental results. Two main catalytic species are observed in reasonable concentrations. One of them is the complex PhPd(SR)(dppf) (**4**) which is the major complex up to about 82% conversion (t = 95000 s in Figures 4a and 4b), which is indeed consistent with the reductive elimination reaction controlling the rate of the catalytic reaction up to this stage. The second observable catalytic species is the Pd^0 complex Pd^0(dba)(dppf) whose concentration is less than that of **4** up to 82% conversion (t = 95000 s in Figure 4b). It then becomes the major complex, which means that the oxidative addition reaction becomes rate-limiting at the very end of the catalytic reaction. This simulation is in agreement with our above proposal. An induction period is observed for the formation of the coupling product **2** at the very beginning of the catalytic reaction ($t < 1000$ s) (enlargement of Figure 4a, not shown), which is consistent with the accumulation of complex **4** that occurs in a slow reductive elimination reaction. We also observe that the protonated amine $HNEt_3^+$, which is generated in a faster deprotonation step, is produced before the coupling product **2** at the very beginning of the reaction (Figure 4a).

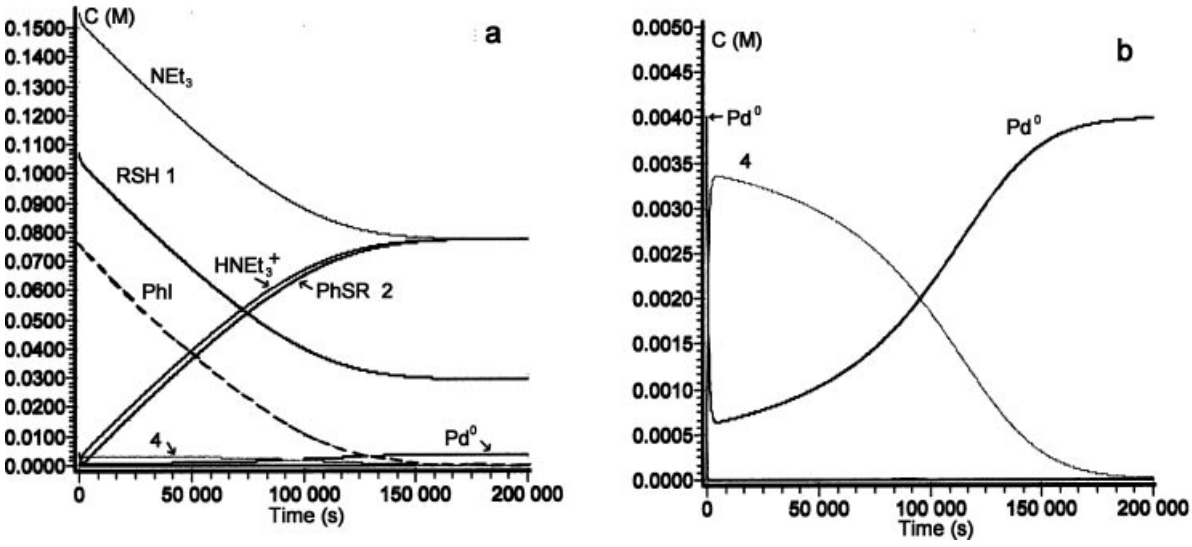

Figure 4. a) Simulation of the concentration profiles of the reagents, products and catalytic species in the catalytic reaction (Scheme 3) against time using the initial concentrations of PhI (77.7 mM), NEt_3 (155 mM), RSH **2** (107 mM) and Pd^0 (4 mM) of the catalytic reaction and the rate constants determined in this work in acetone at 25 °C.[15] b) Concentration profiles of the catalytic species obtained from Figure 4a in the concentration range 0–5 mM (the concentration profiles of the reagents and products have been withdrawn for more clarity).

The oxidative addition reaction may also limit the rate of the catalytic cycle if a less reactive reagent such as PhBr is used. Indeed, the ^{31}P NMR spectrum resulting from the addition of PhBr (1 equiv.) to a mixture of $Pd_2(dba)_3{\cdot}CHCl_3$ (6.6 mM) and dppf (Pd/dppf = 1:1) in [D_6]acetone at room temperature showed, after 17 h, just the two doublets of the unreactive Pd^0(dba)(dppf). Additional doublets which would have characterized PhPdBr(dppf) were not detected. This result is in agreement with the fact that the catalytic cross-coupling reaction between PhBr and the cysteine-derived thiol **1** did not occur under the experimental conditions used for the reaction with PhI[2] because the oxidative addition of PhBr was too slow.

Rate and Mechanism of the Reaction between PhPdI(dppf) and the Cysteine-Derived Thiol 1 in the Presence of Propylene Oxide in Acetone

As reported already, the catalytic cross-coupling reaction between PhI and the cysteine-derived thiol **1** (Scheme 3) was also performed in the presence of propylene oxide as the probase instead of NEt_3. The catalytic reaction was however less efficient.[2] Propylene oxide (10 equiv.) and the thiol **1** (5 equiv.) were added to the complex **3** (13.3 mM) generated in situ by reacting PhI with $Pd_2(dba)_3{\cdot}CHCl_3$ and dppf (Pd/dppf/PhI = 1:1:1) in [D_6]acetone. The formation of **4**, followed by ^{31}P NMR spectroscopy, was extremely slow, much slower than in the presence of NEt_3 and the thiol **1**, even when used in lower concentrations (1 equiv. each) as described above. To be able to deprotonate complexes **5**, the propylene oxide must be opened by a nucleophile, I^- being the only one available (Scheme 13). In acetone, a poorly dissociative solvent, the dissociation of I^- must be an endergonic process; this is why the metallation of **1** was so slow. It was indeed accelerated when the reaction was performed in the presence of 10 equiv. of I^- introduced as nBu_4NI.

Mechanism of the Palladium-Catalyzed Cross Coupling Reaction of Vinyl Iodides with Cysteine-Derived 1

It has been established by some of us that the cross-coupling reaction of the vinyl iodide **8** with the cysteine-derived thiol **1** was efficient when performed in NMP at 70 °C with NEt_3 as the base (Scheme 14). No coupling product was obtained in refluxing acetone.[2]

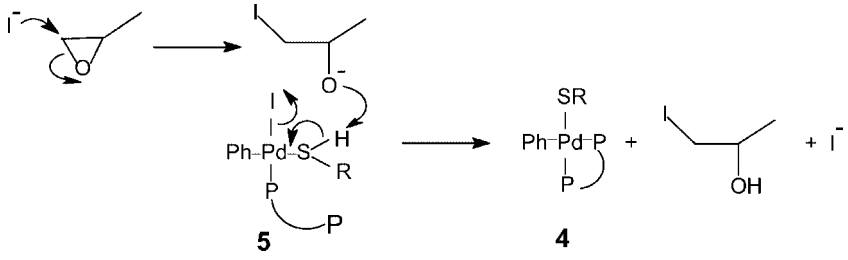

Scheme 13. Tentative mechanism for the metallation of the thiol **1** induced by a probase.

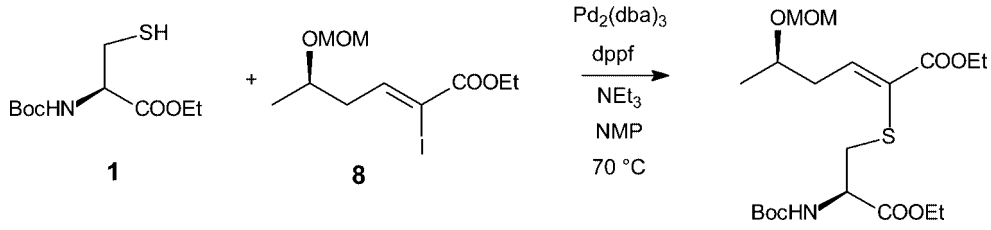

Scheme 14. Palladium-catalyzed coupling reaction of the vinyl iodide **8** with the cysteine-derived thiol **1**.

The mechanism of this cross-coupling reaction was investigated in acetone at 25 °C in an effort to understand why it did not occur in this solvent. When the vinyl iodide **8** (1 equiv.) was added to the complex Pd^0(dba)(dppf) (13.3 mM) generated in a solution of $Pd_2(dba)_3{\cdot}CHCl_3$ and dppf (Pd/dppf = 1), a slow oxidative addition reaction took place.[16,17] The two ^{31}P NMR doublets characteristic of Pd^0(dba)(dppf) (vide supra) totally disappeared only after 120 min. Two new sets of two doublets of equal magnitude were then observed, characterizing two different vinyl-palladium(II) complexes that formed in equal amounts: one set at 9.1 (d, J_{PP} = 31 Hz, 0.5 P) and 27.4 ppm (d, J_{PP} = 31 Hz, 0.5 P) and the other one at 9.4 (d, J_{PP} = 31 Hz, 0.5 P) and 28.0 ppm (d, J_{PP} = 31 Hz, 0.5 P). The two complexes have the same J_{PP} coupling constant, suggesting two diastereomeric complexes, **9** and **10** (Scheme 15).

In the case of the bulky vinyl iodide **8**, the rotation around the C–Pd axis is restricted as a result of steric hindrance, which generates atropisomeric enantiomers at the palladium center. As the vinyl moieties have a chiral group, two diastereoisomers are formed, as observed by Elsevier and co-workers[18] with η^1-allenyl complexes *cis*-[Me-C(Et)=C=CH–PdBr$(PPh_3)_2$].[19a]

By addition of NEt_3 (5 equiv.) and the thiol derived from the enantiomerically pure cysteine **1** (5 equiv.) to the solution containing complexes **9** and **10** (13.3 mM) in acetone, a reaction took place since the two sets of two doublets started to disappear although at different rates. This is further evidence of the diastereoisomeric character of complexes **9** and **10**. The diastereoisomer characterized by the two doublets at 9.1 and 27.4 ppm was the most reactive one.[20] Neither of them was detected after 60 min. Instead, two new sets of two doublets of equal magnitude with the same J_{PP} coupling constant were detected, one at δ = 14.8 (d, J = 32 Hz, 0.5 P) and 25.6 ppm (d, J = 32 Hz, 0.5 P), the second at δ = 15.0 (d, J = 32 Hz, 0.5 P) and 25.9 ppm (d, J = 32 Hz, 0.5 P). They characterize the transmetallation complexes **11** and **12** which are also diastereomeric com-

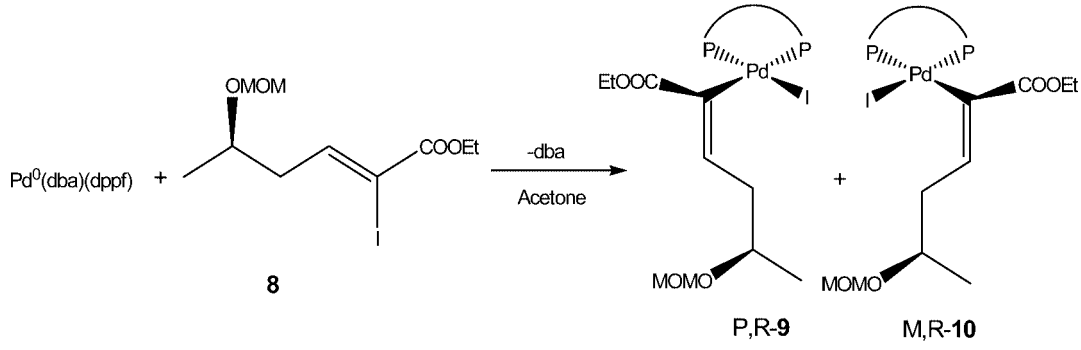

Scheme 15. Formation of diastereoisomers in the oxidative addition reaction of the chiral vinyl iodide **8**.

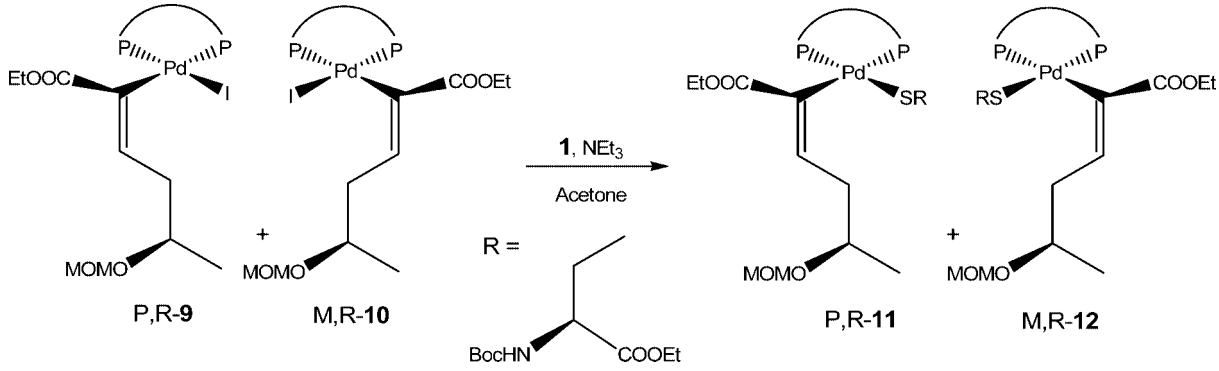

Scheme 16. Formation of diastereomeric complexes **11** and **12** (P–P = dppf).

plexes (Scheme 16). These complexes were very stable ($t >$ 15 h) and no reductive elimination took place in acetone at room temperature.[19b,19c]

From this qualitative study, one can assume that under our experimental conditions oxidative addition and metallation of the thiol took place in acetone at 25 °C, whereas the reductive elimination reaction did not, which is of the reason for the low efficiency of the catalytic reaction in acetone. Reductive elimination reactions from vinyl-palladium complexes are usually faster than those from aryl-palladium complexes.[9a,21] The reverse situation was observed in this work. This is probably due to the COOEt group which stabilizes complexes **11** and **12** by steric hindrance, as observed in *ortho*-substituted diaryl-nickel complexes,[22] and by its electron-withdrawing properties which disfavor the reductive elimination reaction.[22]

Conclusions

The mechanism of the palladium-catalyzed cross-coupling reaction of aryl or vinyl halides with a cysteine-derived thiol **1** (RSH) has been established by the characterization of all the palladium complexes involved in the catalytic cycle, namely, Pd^0(dba)(dppf), R′PdI(dppf), R′PdI(SHR)(η^1-dppf) and R′PdI(SR)(dppf) (R′ = aryl or vinyl). The kinetics of the oxidative addition, metallation and reductive elimination reactions in which they are involved, have been investigated, each step considered independently of each other, using the initial reagent concentrations used in the catalytic reaction. The classic transmetallation of R′PdI(dppf) by RS^-, even if generated in very low concentrations, cannot entirely be excluded. However the detection of the complex PhPdI(SHR)(η^1-dppf) leads us to propose an alternative mechanism. The metallation of the thiol proceeds in two steps: reversible complexation of the thiol to form PhPdI(SHR)(η^1-dppf) after decomplexation of one of the phosphorus atoms of the dppf ligand (Scheme 12) followed by the easier deprotonation of the ligated RSH by the base or the probase. This alternative mechanism would take place with weakly acidic thiols, for which the formation of RS^- is very endergonic.

As far as phenyl iodide is concerned, and in conditions similar to those of the catalytic cycle (same solvent: acetone; same catalytic precursor: $Pd_2(dba)_3{\cdot}CHCl_3$ and dppf; same base: NEt_3; and similar initial reagent concentrations),[2] it has been established from the kinetic data that the reductive elimination reaction is intrinsically the slowest step (Scheme 12) up to 82% conversion. When propylene oxide is used as the probase, the metallation of the thiol becomes the slowest step which can be accelerated upon addition of iodide ions.

The cross-coupling reaction of PhBr performed under the same experimental conditions failed.[2] It has been established in this work that the oxidative addition reaction is very slow. The cross-coupling reaction of the vinyl iodide **8** with RSH **1** did not occur in acetone.[2] The mechanistic study performed in acetone shows that the oxidative addition and metallation of **1** proceeded more slowly with a vinyl iodide than with an aryl iodide when investigated independently using similar reagent concentrations. The reductive elimination from vinyl–Pd(SR)(dppf) did not proceed at all at room temperature. Interestingly, diastereoisomeric complexes vinyl–PdX(dppf) (X = I, SR) were formed owing to the atropisomerism induced by the bulkiness of the investigated vinyl group and its chirality or that of the SR group.

Experimental Section

All experiments were performed using standard Schlenk techniques under argon. The ^{31}P NMR spectra were recorded in degassed [D_6]acetone with a Bruker spectrometer (101 MHz) (Avance 250) using H_3PO_4 as an external reference; the ^{1}H NMR spectra were recorded with a Bruker spectrometer (250 MHz). Cyclic voltammetry and amperometry were performed with a home-made potentiostat and a wave-form generator GSTP4 (Radiometer analytical). The current was recorded with a Nicolet 301 oscilloscope.

Materials: Phenyl iodide, phenyl bromide and triethylamine were obtained commercially and used after filtration through alumina. Propylene oxide and dppf were obtained commercially and used as received. The cysteine-derived thiol **1**,[2] the vinyl iodide **8**,[2] $Pd_2(dba)_3{\cdot}CHCl_3$[23] and PhPdI(PPh_3)[24] were synthesized as reported in literature.

General Procedure for Determining the Kinetics of the Oxidative Addition Reaction of PhI as Monitored by Amperometry: Experiments were carried out in a three-electrode thermostatted cell connected to a Schlenk line. The counter electrode was a platinum wire with an apparent surface area of about 1 cm^2; the reference was a saturated calomel electrode (Radiometer Analytical) separated from the solution by a bridge (3 mL) filled with a 0.3 M $n$$Bu_4NBF_4$ solution in acetone. Degassed acetone (15 mL) containing 0.3 M $n$$Bu_4NBF_4$ was poured into the cell. $Pd_2(dba)_3{\cdot}CHCl_3$ (31 mg, 30 μmol, 2 mM) was then introduced into the cell followed by dppf (32 mg, 60 μmol, 4 mM). The kinetic measurements were performed at a rotating gold disk electrode (d = 2 mm, inserted into a Teflon holder, EDI 65109, Radiometer Analytical) with an angular velocity of 105 rad s^{-1} (Radiometer Analytical controvit). The rotating electrode was polarized at +0.55 V on the plateau of the oxidation wave of Pd^0(dba)(dppf). Phenyl iodide (130 μL, 1.16 mmol) was then added to the cell and the decrease in the oxidation current was recorded versus time up to 100% conversion.

General Procedure for the Oxidative Addition Reaction, as Monitored by ^{31}P NMR Spectroscopy: dppf (5.5 mg, 0.01 mmol) was added to a solution of $Pd_2dba_3{\cdot}CHCl_3$ (5.2 mg, 0.005 mmol) in degassed [D_6]acetone (0.75 mL). The ^{31}P NMR spectrum exhibited the two doublets of Pd^0(dba)(dppf).[7b] PhI (1.2 μL, 0.011 mmol) was then introduced and the ^{31}P NMR spectrum exclusively exhibited the two doublets of PhPdI(dppf) (**3**)[7b] which was generated in quantitative yield.

The experiments involving PhBr or the vinylic iodide **8** were performed similarly using the concentrations reported earlier in the text.

General Procedure for the Metallation of the Thiol 1, as Monitored by ^{31}P NMR Spectroscopy: NEt_3 (1.4 μL, 0.01 mmol) was added to PhPdI(dppf) (**3**, 0.01 mmol) generated as above. ^{31}P NMR spectra were recorded at different times and indicated that no reaction occurred. The cysteine-derived thiol **1** (2.4 μL, 0.01 mmol) was then added and again ^{31}P NMR spectra were recorded at different times.

The first spectrum recorded after 20 min exhibited the two doublets of PhPd(SR)(dppf) (**4**) whose structure was confirmed by ^{1}H NMR spectroscopy. In another experiment, propylene oxide was used instead of NEt_3.

The experiments involving the complexes **11** and **12** generated from the vinylic iodide **8** were performed similarly using NEt_3 and **1** in concentrations reported earlier in the text.

Procedure for the Detection of the Intermediate Complex PhPdI(RSH)(η^1-dppf) (5) by ^{31}P NMR Spectroscopy: Cysteine-derived thiol **1** (60 μL, 0.25 mmol) was added twice to a solution of PhPdI(dppf) (**3**) generated after addition of PhI (1.2 μL, 0.011 mmol) to a solution of Pd(dba)(dppf), which was formed in situ by reacting $Pd_2dba_3{\cdot}CHCl_3$ (5.2 mg, 0.005 mmol) and dppf (5.5 mg, 0.01 mmol) in degassed [D$_6$]acetone (0.75 mL). A ^{31}P NMR spectrum was recorded after each addition of **1**.

General Procedure for the Kinetics of the Reductive Elimination Reaction as Monitored by ^{31}P NMR Spectroscopy in Acetone: Once the complex PhPd(SR)(dppf) (**4**, 13.3 mM) had been generated in the "transmetallation" step as described above, ^{31}P NMR spectra were recorded at different times after the introduction of H_3PO_4 (85% in water), as internal standard, into a capillary tube until **4** totally disappeared. The evolution of the magnitude of one doublet of **4** (at 13.4 ppm) was compared to the magnitude of the singlet of H_3PO_4.

Characterization of the Palladium Complexes involved in the Catalytic Cycle: The complexes generated in all the steps of the catalytic reaction were characterized in situ. Indeed, our objective was to investigate the kinetics of each step, one step after the other, to fit the experimental conditions of the catalytic reaction and to take into account all the components of the catalytic reaction (e.g., dba which is present in every step because it is delivered by the precursor $Pd_2(dba)_3$). However, some complexes could not be isolated: **4** (undergoing a reductive elimination at 25 °C) and **5** (generated at a low concentration in an endergonic equilibrium) (vide infra).

[Pd(Ph$_2$P{(C$_5$H$_4$)$_2$Fe}PPh$_2$)(Ph)(I)] (3): Complex **3** observed in situ was identical to an authentic sample:[7b] ^{1}H NMR (250 MHz, [D$_6$]-acetone): δ = 3.72 ("d", J = 1.5 Hz, 2 H, Cp), 4.27 (m, 2 H, Cp), 4.61 (m, 2 H, Cp), 4.82 ("d", J = 1.5 Hz, 2 H, Cp), 6.38 (m, 1 H, *p*-H of Ph), 6.46 ("t", J = 7 Hz, 2 H, *m*-H of Ph), 6.93 (dd, J = 8, J_{PH} = 8 Hz, 2 H, *o*-H of Ph), 7.20–7.26 (m, 4 H, H of PPh_2), 7.42–7.45 (m, 4 H, H of PPh_2), 7.55–7.56 (m, 8 H, H of PPh_2), 8.10–8.20 (m, 4 H, H of PPh_2) ppm. ^{31}P NMR (101 MHz, [D$_6$]acetone): δ = 7.7 (d, J = 34 Hz, 1 P), 26.2 (d, J = 34 Hz, 1 P) ppm.

[Pd(Ph$_2$P{(C$_5$H$_4$)$_2$Fe}PPh$_2$){SCH$_2$CH(NHBoc)(COOEt)}(Ph)] (4): Complex **4** was observed in situ. It could not be isolated as a pure compound because it underwent spontaneous reductive elimination at 25 °C. ^{1}H NMR (250 MHz, [D$_6$]acetone): δ = 1.28 (t, J = 7 Hz, 3 H), 1.4 (s, 9 H), 3.33 (dd, J = 14, J = 7.7 Hz, 1 H), 3.47 (dd, J = 14, J = 5 Hz, 1 H), 3.72 (~d, J = 1.5 Hz, 2 H), 4.10 (m, 2 H), 4.27 (m, 2 H), 4.61 (m, 2 H), 4.82 (~d, J = 1.5 Hz, 2 H), 6.38 (m, 1 H), 6.46 (~t, J = 7 Hz, 2 H), 6.93 (dd, J = 8, J_{PH} = 8 Hz, 2 H), 7.20–7.26 (m, 4 H), 7.42–7.45 (m, 4 H), 7.55–7.56 (m, 8 H), 8.10–8.20 (m, 4 H) ppm. ^{31}P NMR (101 MHz, [D$_6$]acetone): δ = 13.4 (d, J = 31 Hz, 1 P), 23.4 (d, J = 31 Hz, 1 P) ppm. The protonated triethylamine $HNEt_3^+$ was also observed: ^{1}H NMR (250 MHz, [D$_6$] acetone): δ = 1.28 (t, J = 7 Hz, 3 H), 2.96 (q, J = 7 Hz, 2 H) ppm.

[Pd(η^1-Ph$_2$P{(C$_5$H$_4$)$_2$Fe}PPh$_2$){HSCH$_2$CH(NHBoc)(COOEt)}(Ph)(I)] (5): Complex **5** could not be isolated because it was generated in an endergonic equilibrium with HSCH$_2$CH(NHBoc)(COOEt). It was therefore observed in situ. ^{31}P NMR (101 MHz, [D$_6$]acetone): δ = –17.9 (s, 1P), 18.7 (s, 1P) ppm. Its ^{1}H NMR signals could not be observed because **5** was generated in the presence of a large excess (25 or 50 equiv.) of HSCH$_2$CH(NHBoc)(COOEt) thus saturating the ^{1}H NMR spectrum.

[Pd(Ph$_2$P{(C$_5$H$_4$)$_2$Fe}PPh$_2$){C(COOEt)CHC$_2$H$_3$(OMOM)(CH$_3$)}(I)] (9 and 10): ^{1}H NMR (250 MHz, [D$_6$]acetone) the signals selected here are those that show that two diastereoisomers were formed: δ = 1.06 (d, J = 6.2 Hz, 1.5 H, Me(6)), 1.15 (d, J = 6.1 Hz, 1.5 H, Me(6)), 3.23 (s, 1.5 H, Me(MOM)), 3.36 (s, 1.5 H, Me(MOM)), 4.08 (br. s, 2 H), 4.24 (br. s, 2 H), 4.31 (br. s, 2 H), 4.70 (br. s, 2 H), 6.10–6.20 (m, 1 H, C=CH), 7.20–7.27 (m, 4 H), 7.52–7.60 (m, 12 H), 8.07–8.20 (m, 4 H) ppm. ^{31}P NMR (101 MHz, [D$_6$]-acetone): δ = 9.1 (d, J = 31 Hz, 0.5 P), 27.4 (d, J = 31 Hz, 0.5 P), 9.4 (d, J = 31 Hz, 0.5 P), 28.0 (d, J = 31 Hz, 0.5 P) ppm.

[Pd(Ph$_2$P{(C$_5$H$_4$)$_2$Fe}PPh$_2$){SCH$_2$CH(NHBoc)(COOEt)}{C(COOEt)CHC$_2$H$_3$(OMOM)(CH$_3$)}] (11 and 12): ^{1}H NMR (250 MHz, [D$_6$]acetone) the signals selected here are those that show that two diastereoisomers were formed: δ = 3.25 (s, 1.5 H, Me(MOM)), 3.37 (s, 1.5 H, Me(MOM)) ppm. ^{31}P NMR (101 MHz, [D$_6$]acetone): δ = 14.8 (d, J = 32 Hz, 0.5 P), 25.6 (d, J = 32 Hz, 0.5 P), 15.0 (d, J = 32 Hz, 0.5 P), 25.9 (d, J = 32 Hz, 0.5 P) ppm.

Acknowledgments

This work has been supported by the Centre National de la Recherche Scientifique (UMR CNRS-ENS-UPMC 8640, UPR 2301) and the Ministère de la Recherche (Ecole Normale Supérieure). The Ministère de la Recherche is also thanked for a grant (X. M.).

[1] X. Moreau, J. M. Campagne, *J. Org. Chem.* **2003**, *68*, 5346–5350.
[2] X. Moreau, J. M. Campagne, *J. Organomet. Chem.* **2003**, *687*, 322–326.
[3] For the seminal use of the dppf ligand in C–S coupling reactions, see: P. G. Ciattini, E. Morera, G. Ortar, *Tetrahedron Lett.* **1995**, *36*, 4133–4136.
[4] For the formation of C–S bonds by palladium-catalyzed cross-coupling reactions, see also: a) M. Kosugi, T. Shimizu, T. Migita, *Chem. Lett.* **1978**, 13–14; b) I. W. J. Still, F. D. Toste, *J. Org. Chem.* **1996**, *61*, 7677–7680; c) S. Rajagopalan, G. Radke, M. Evans, J. M. Tomich, *Synth. Commun.* **1996**, *26*, 1431–1440; d) S. Wendeborn, S. Berteina, W. K. D. Brill, A. De Mesmaeker, *Synlett* **1998**, 671–675; e) G. Y. Li, *J. Org. Chem.* **2002**, *67*, 3643–3650; f) P. Prim, J. M. Campagne, D. Joseph, B. Andrioletti, *Tetrahedron* **2002**, *58*, 2041–2075.
[5] For recent reviews on the formation of C–S bonds using copper-catalyzed reactions, see: a) S. V. Ley, A. W. Thomas, *Angew. Chem. Int. Ed.* **2003**, *42*, 5400–5449; b) K. Kunz, U. Scholz, D. Ganzer, *Synlett* **2003**, 2428–2439.
[6] a) C. Amatore, A. Jutand, *J. Organomet. Chem.* **1999**, *576*, 254–278; b) A. Jutand, *Pure Appl. Chem.* **2004**, *76*, 565–576; c) In a catalytic cycle, the rate of step i is given by rate$_i$ = k_i[R$_i$][M$_i$] (where k_i is the rate constant, [R$_i$] the concentration of the reagent R$_i$ involved in the elemental step I and [M$_i$] the concentration of the reactive catalytic species M$_i$). The concentration of M$_i$ is controlled by the rate of the previous reaction (i – 1) in which M$_i$ is generated.
[7] a) Pd(dba)$_2$ is the usual formula given in the literature, see ref.[23]; b) C. Amatore, G. Broeker, A. Jutand, F. Khalil, *J. Am. Chem. Soc.* **1997**, *119*, 5176–5185.
[8] a) The overall oxidative addition reaction is a complex mechanism (see Scheme 5) that involves an equilibrium constant (i.e., two rate constants) and two rate constants that characterize the oxidative addition reactions of Pd^0(dba)dppf and SPd^0(dppf). Only two rate constants could be determined, as

reported in ref.[7b]. The apparent rate constant of the overall oxidative addition reaction was calculated from the equation $k_{obs}^{add.ox.} = k_{app}^{add.ox.}$[PhI] (with [PhI] = 77.3 mM), which gives $k_{app}^{add.ox.} = 0.017\ M^{-1}s^{-1}$ ([Pd^0] = 4 mM, acetone, 30 °C); b) in the catalytic reactions reported by some of us,[2] and by Ortar and co-workers,[3] a ratio of dppf/Pd of 2 was used instead of 1 as in the present work. The complexes generated in situ from $Pd^0(dba)_2$ and dppf (2 equiv.) were characterized in previous work.[7b] Initially a fast reaction quantitatively affords Pd^0(dba)(dppf). At much longer reaction times, a slow reaction occurs between Pd^0(dba)(dppf) and dppf to give $Pd^0(dppf)_2$. In THF, the formation of $Pd^0(dppf)_2$ required 22 h starting from $Pd^0(dba)_2$ (2 mM) and dppf (4 mM) at room temperature;[7b] moreover, an oxidative addition reaction was not observed between PhI (200 mM) and $Pd^0(dppf)_2$ (2 mM) at room temperature;[7b] Consequently, in the catalytic reactions, the oxidative addition of Pd^0(dba)(dppf) to PhI, whose observed rate constant has been determined in this work (see text and Figure 1), proceeds faster than its reaction with the second dppf ligand. In other words, in the catalytic reaction, the kinetics of the oxidative addition reaction will not be perturbed by the presence of the second dppf ligand, except at the very end of the catalytic reaction when the concentration of PhI is very low.

[9] a) G. Mann, D. Baranano, J. F. Hartwig, A. L. Rheingold, I. A. Guzei, *J. Am. Chem. Soc.* **1998**, *120*, 9205–9219; b) J. F. Hartwig, *Acc. Chem. Res.* **1998**, *31*, 852–860.

[10] M. R. Crampton in *The Chemistry of the Thiol Group* (Ed.: S. Patai), Wiley, London, **1974**, pp. 396–398.

[11] a) By considering the steady-state approximation for complex PhPdI(RSH)(η^1-dppf), the expression for the observed rate constant for the transmetallation process is $k_{obs}^{"met."} = Kk[NEt_3][RSH]$ (k is the rate constant for the reaction of NEt_3 with PhPdI(RSH)(η^1-dppf) with a first-order reaction in NEt_3 and RSH). If the steady-state approximation cannot be applied because complex PhPdI(RSH)(η^1-dppf) accumulates in solution, then the expression for the observed rate constant for the transmetallation reaction is $k_{obs}^{"met."} = Kk[NEt_3][RSH]/(1 + K[RSH])$. With an initial RSH concentration of 107 mM, as in the catalytic reaction, and with $K = 0.4\ M^{-1}$, as determined in this work (see text), one obtains K[RSH] = 0.04, which is negligibly smaller than 1. The expression of $k_{obs}^{"met."}$ is then similar to the former one expressed above; b) A minimum value of $k > 28\ M^{-1}s^{-1}$ was estimated from the value of $k_{obs}^{"met."} = Kk[NEt_3][RSH]$,[11a] with $k_{obs}^{"met."} > 5 \times 10^{-3}\ s^{-1}$ determined experimentally for [NEt_3] = [RSH] = 13.3 mM and $K = 0.4\ M^{-1}$. The value of $k_{obs}^{"met."}$ will be about 90 times higher when considering the initial NEt_3 and RSH concentrations (155 mM and 107 mM, respectively) used in the catalytic reactions than for the concentrations investigated here (13.3 mM each); c) A value of $k = 28\ M^{-1}s^{-1}$ was used to simulate the kinetics of the catalytic reaction (see Figure 4).[15] Since $K = k_+/k_- = 0.4\ M^{-1}$, the rate constants for the forward and backward reactions were considered to be $k_+ = 40\ M^{-1}s^{-1}$ and $k_- = 100\ s^{-1}$, respectively, in order to simulate the kinetics of the catalytic reaction.[15]

[12] a) J. Louie, F. Paul, J. F. Hartwig, *Organometallics* **1996**, *15*, 2794–2805; b) U. K. Singh, E. R. Strieter, D. G. Blackmond, S. L. Buchwald, *J. Am. Chem. Soc.* **2002**, *124*, 14104–14114; c) F. Ozawa, N. Kawasaki, H. Okamoto, T. Yamamoto, A. Yamamoto, *Organometallics* **1987**, *6*, 1640–1651.

[13] In ref.[9a], Hartwig and co-workers discussed the effect of trapping agents of Pd^0 on the reaction rate of the reductive elimination reaction, which may be positive or negative. In our present study, dba acts as the trapping agent for the Pd^0 complex generated in the reductive elimination reaction (see Scheme 11). However, since dba is always present in the catalytic reaction as it is introduced by the precursor $Pd_2(dba)_3$, we did not try to investigate the effect of dba on the reductive elimination rate to fit the conditions of the catalytic reactions.

[14] a) The rate of the reductive elimination is given by $rate^{red.elim.} = k^{red.elim.}$[**4**]. It depends only on the concentration of **4**. When investigated independently of the previous reactions, the rate of this reaction does not depend on the concentrations of the other reagents of the catalytic reaction. But in the course of the catalytic reaction, the concentration of **4** will depend on the kinetics of the previous reactions; b) in this work, the observed rate constant for the oxidative addition reaction, $k_{obs}^{add.ox.}$ (in s^{-1}), was determined for the initial concentration of PhI used in the catalytic reaction to compare the rate of the oxidative addition, $rate^{add.ox.} = k_{obs}^{add.ox.}$[$Pd^0$], with that of the individual subsequent steps for [Pd^0] = [**3**] = [**4**]; c) the observed rate constant for the metallation of **1**, $k_{obs}^{"met."}$ (in s^{-1}), was determined independently of the preceding oxidative addition reaction for a given concentration of NEt_3 and **1** (see text and ref.[11b]) to compare the metallation rate, $rate^{"met."} = k_{obs}^{"met."}$[**3**], with that of the individual previous and subsequent steps for [Pd^0] = [**3**] = [**4**]; d) $k^{red.elim.} = k_{app}^{add.ox.}$[PhI] = $2.3 \times 10^{-4}\ s^{-1}$ when [PhI] = 13.5 mM, corresponding to 82% conversion.

[15] Scheme used to simulate the catalytic reaction:

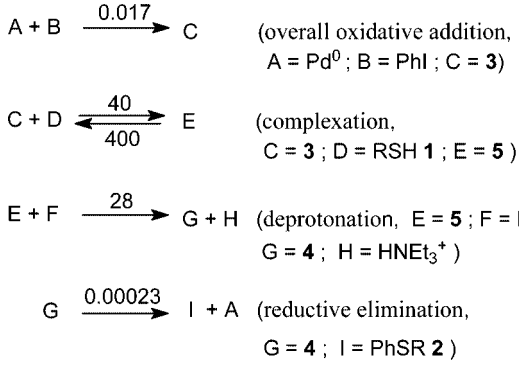

Initial concentrations: $[A]_0$ = 4 mM; $[B]_0$ = 77.3 mM; $[D]_0$ = 107 mM; $[F]_0$ = 155 mM; $[C]_0 = [E]_0 = [G]_0 = 0$.

[16] For oxidative addition of vinyl halides to Pd^0 complexes ligated by dppf, see: J. M. Brown, N. A. Cooley, *J. Chem. Soc., Chem. Commun.* **1988**, 1345–1347.

[17] The oxidative addition reaction of the vinyl iodide **8** was slower than that of PhI under similar concentrations. This unusual reactivity order is probably due to the steric hindrance of the vinyl iodide. Indeed, the iodide and the chain are in a *cis* position, thus preventing an easy complexation of the Pd^0 moieties to the C=C bond which takes place before C–I activation.[16] See also: A. Jutand, S. Négri, *Organometallics* **2003**, *22*, 4229–4237.

[18] J. M. A. Wouters, R. A. Klein, C. J. Elsevier, L. Häming, C. H. Stam, *Organometallics* **1994**, *13*, 4586–4593.

[19] a) This assumption was confirmed by performing the oxidative addition reaction with the related vinylic iodide possessing an achiral *n*-propyl chain. Only one set of two doublets was observed, indicating that only atropisomeric enantiomers were generated. [$Pd(Ph_2P\{(C_5H_4)_2Fe\}PPh_2)\{C(COOEt)CH(C_3H_7)\}$-(I)]: ^{1}H NMR (250 MHz, [D_6]acetone): δ = 0.90 (t, J = 7.3 Hz, 3 H), 1.13–1.18 (m, 1 H), 1.23 (t, J = 7.2 Hz, 3 H), 1.26–1.32 (m, 1 H), 1.98 (br. m, 2 H), 3.96–4.01 (m, 2 H), 4.06 (br. s, 2 H), 4.21 (br. s, 2 H), 4.56 (br. s, 2 H), 4.66 (br. s, 2 H), 6.11 (m, 1 H, C=CH), 7.18–7.25 (m, 4 H), 7.53–7.66 (m, 12 H), 8.07–8.15 (m, 4 H) ppm. ^{31}P NMR (101 MHz, [D_6]acetone): δ = 9.0 (d, J = 31 Hz, 1 P), 27.7 (d, J = 31 Hz, 1 P) ppm; b) When the latter complexes were reacted with NEt_3 (5 equiv.) and the thiol (*R*)-**1** (5 equiv.), two sets of two doublets were observed with the same J_{PP} coupling constant. Two diastereoisomers were then generated as a result of the atropisomerism induced by the hindered rotation along the Pd–C axis and the chirality of the RS group. These complexes were stable at room temperature in acetone and did not undergo any reductive elimination. [$Pd(Ph_2P\{(C_5H_4)_2Fe\}PPh_2)\{SCH_2CH(NHBoc)$-

(COOEt)}{C(COOEt)CH(C_3H_7)}]: ^{31}P NMR (101 MHz, [D_6]-acetone): δ = 14.4 (d, J = 32 Hz, 0.5 P), 25.6 (d, J = 32 Hz, 0.5 P). 14.7 (d, J = 32Hz, 0.5 P), 25.6 (d, J = 32 Hz, 0.5 P) ppm; c) It has been checked that the reaction of the enantiomeric complexes generated as in ref.[19a] with the simple achiral thiol ($EtOOCCH_2SH$) in the presence of NEt_3 gave only two stable enantiomeric complexes [{*n*PrCH=C(CO_2Et)}Pd{SCH_2-(CO_2Et)}(dppf)] that are characterized by a unique set of two ^{31}P NMR doublets at δ = 15.3 (d, J_{PP} = 31 Hz, 1 P) and 25.7 ppm (d, J_{PP} = 31 Hz, 1 P), providing evidence that the diastereoisomers observed in this work (complexes **9** and **10**, **11** and **12**, and those described in ref.[19b]) were indeed the results of an atropisomerism due to the bulkiness of the vinyl group and associated with the chirality of the vinyl chain and/or that of the R group of the cysteine-derived thiol **1**.

[20] Since one diastereoisomer was more reactive than the other, the two sets of doublets could be distinguished, the doublets gathered two by two and assigned to either **9** or **10**.
[21] J. M. Brown, P. J. Guiry, *Inorg. Chim. Acta* **1994**, *220*, 249–259.
[22] J. Chatt, B. L. Shaw, *J. Chem. Soc.* **1960**, 1719–1723.
[23] Y. Takahashi, T. I. Ito, Y. Ishii, *J. Chem. Soc., Chem. Commun.* **1970**, 1065–1070.
[24] P. Fitton, M. P. Johnson, J. E. McKeon, *J. Chem. Soc., Chem. Commun.* **1968**, 6–7.

Received: March 30, 2005
Published Online: July 12, 2005

